Cell, Vol. 119, 19–31, October 1, 2004, Copyright ©2004 by Cell Press

$Ca_V1.2$ Calcium Channel Dysfunction Causes a Multisystem Disorder Including Arrhythmia and Autism

Igor Splawski,[1,*] Katherine W. Timothy,[2] Leah M. Sharpe,[1] Niels Decher,[3] Pradeep Kumar,[3] Raffaella Bloise,[4] Carlo Napolitano,[4] Peter J. Schwartz,[5,6] Robert M. Joseph,[7] Karen Condouris,[7] Helen Tager-Flusberg,[7] Silvia G. Priori,[4,5] Michael C. Sanguinetti,[3] and Mark T. Keating[1]

[1]Department of Cardiology
Children's Hospital
Departments of Pediatrics and Cell Biology
Harvard Medical School and
Howard Hughes Medical Institute
Boston, Massachusetts 02115
[2]Department of Human Genetics and
[3]Department of Physiology and Nora Eccles Harrison Cardiovascular Research and Training Institute
University of Utah
Salt Lake City, Utah 84112
[4]Department of Molecular Cardiology
IRCCS Fondazione Salvatore Maugeri
[5]Department of Cardiology
University of Pavia
[6]IRCCS Policlinico San Matteo
27100 Pavia
Italy
[7]Department of Anatomy and Neurobiology
Boston University School of Medicine
Boston, Massachusetts 02118

Summary

$Ca_V1.2$, the cardiac L-type calcium channel, is important for excitation and contraction of the heart. Its role in other tissues is unclear. Here we present Timothy syndrome, a novel disorder characterized by multiorgan dysfunction including lethal arrhythmias, webbing of fingers and toes, congenital heart disease, immune deficiency, intermittent hypoglycemia, cognitive abnormalities, and autism. In every case, Timothy syndrome results from the identical, de novo $Ca_V1.2$ missense mutation G406R. $Ca_V1.2$ is expressed in all affected tissues. Functional expression reveals that G406R produces maintained inward Ca^{2+} currents by causing nearly complete loss of voltage-dependent channel inactivation. This likely induces intracellular Ca^{2+} overload in multiple cell types. In the heart, prolonged Ca^{2+} current delays cardiomyocyte repolarization and increases risk of arrhythmia, the ultimate cause of death in this disorder. These discoveries establish the importance of $Ca_V1.2$ in human physiology and development and implicate Ca^{2+} signaling in autism.

Introduction

"Ja, Kalzium, das ist alles!" So stated Nobel laureate Otto Loewi in 1959, and it is now clear that Ca^{2+} is the ultimate signaling molecule for organisms ranging from prokaryotes to humans. In higher organisms, Ca^{2+} mediates processes as diverse as synaptic transmission, muscle contraction, insulin secretion, fertilization, and gene expression (Berridge et al., 2003; Brini and Carafoli, 2000; Ren et al., 2001). Because Ca^{2+} cannot be metabolized, cells have evolved complex mechanisms for regulating intracellular Ca^{2+} levels, which are 10,000-fold lower than extracellular levels. Many proteins have been adapted to bind and transport Ca^{2+}, in some cases to reduce Ca^{2+} levels and in others to trigger second-messenger pathways. Excitable cells contain voltage-dependent calcium channels that can dramatically increase cytosolic Ca^{2+}. In heart and brain, the L-type calcium channel $Ca_V1.2$ (*CACNA1C*, α_{1C}, $\alpha_1 1.2$) mediates this process (Catterall, 2000; Mikami et al., 1989; Schultz et al., 1993). By contrast with physiology, the role of Ca^{2+} signaling in development is poorly understood.

The importance and ubiquity of Ca^{2+} as an intracellular signaling molecule suggest that altered channel function could give rise to widespread cellular and organ defects. Previously characterized calcium channel disorders, however, have been marked by dysfunction of a distinct organ system, particularly the membrane excitability of neurons and skeletal muscle. For example, calcium channel syndromes like hypokalemic periodic paralysis and malignant hyperthermia affect skeletal muscle (Monnier et al., 1997; Ptacek et al., 1994), episodic ataxia affects the cerebellum (Ophoff et al., 1996), familial hemiplegic migraine affects vascular smooth muscle (Ophoff et al., 1996), and stationary night blindness affects retina (Bech-Hansen et al., 1998; Strom et al., 1998). None of these disorders has illustrated the full extent of Ca^{2+} signaling in human development and physiology.

Cardiac arrhythmias cause sudden loss of consciousness and sudden death in approximately 1 million Europeans and North Americans every year (Priori et al., 2002; Zheng et al., 2001). Over the last decade, we and others have identified arrhythmia susceptibility genes by studying familial syndromes (Antzelevitch, 2003; Keating and Sanguinetti, 2001). These genes include *SCN5A*, *KVLQT1*, and *HERG*, which encode important cardiac sodium and potassium channels. In the vast majority of arrhythmia syndromes, individuals appear normal except for subtle electrocardiographic abnormalities.

Here, we describe the phenotypic characterization of Timothy syndrome (TS), an arrhythmia disorder associated with dysfunction in multiple organ systems, including congenital heart disease, syndactyly, immune deficiency, and autism. We show that this disorder results from a recurrent, de novo missense mutation in the $Ca_V1.2$ L-type calcium channel gene. The $Ca_V1.2$ gene is expressed in multiple tissues. We demonstrate through functional expression in heterologous systems that the disease-associated mutation causes abnormal Ca^{2+} current. This gain-of-function mechanism is mediated through failed channel inactivation, suggesting that calcium channel blockers may be useful for treating this and related disorders.

*Correspondence: igor@enders.tch.harvard.edu

Results

Timothy Syndrome, a Multisystem Disorder

In 1992, cases of a novel arrhythmia syndrome associated with syndactyly (webbing of fingers and toes) were described (Marks et al., 1995; Reichenbach et al., 1992). We named this disorder Timothy syndrome (TS). Because therapy is extending lives of affected children, we have observed that TS manifests major phenotypic abnormalities of multiple organ systems, including heart, skin, eyes, teeth, immune system, and brain (Figure 1, Table 1).

The inheritance pattern of TS was sporadic in all but one family. In that family, two of three siblings were affected. None of the parents in any of the families was affected. Ten of 17 children with TS died. The average age of death was 2.5 years. All affected individuals had severe prolongation of the QT interval on electrocardiogram, syndactyly, and abnormal teeth and were bald at birth. Arrhythmias were the most serious aspect of this disorder, as 12 of 17 children had life-threatening episodes. Arrhythmic death in two children was triggered by sepsis and in two other children by episodic hypoglycemia. Individuals with this syndrome also had congenital heart disease including patent ductus arteriosus, patent foramen ovale, ventricular septal defects, and tetralogy of Fallot. Some children had dysmorphic facial features, including a flat nasal bridge, small upper jaw, low-set ears, or small and misplaced teeth. Episodic serum hypocalcemia was described in four individuals.

Many of the surviving children showed developmental delays consistent with language, motor, and generalized cognitive impairment. Children had a history of language delay and delay in other motor skills. Many did not produce speech sounds (babbling) during infancy. Testing revealed significant problems in language skills including articulation, reception, and expression. Children were impaired in all areas of adaptive function, including communication, socialization, and daily living skills. Five children were formally evaluated for autism. Three met the criteria for this disorder, one met criteria for autism spectrum disorders, and one had severe delays in language development. We could not evaluate additional children because they were deceased or unavailable. However, the association between autism spectrum disorders and Timothy syndrome was significant ($p = 1.2 \times 10^{-8}$). Taken together, the diversity of these phenotypic abnormalities indicates a complex physiological and developmental disorder.

Recurrent De Novo Missense Mutation in $Ca_V1.2$ Causes TS

The TS phenotype suggested two possible genotypes. The severity of arrhythmias in this disorder suggested a recessive gene knockout similar to Jervell and Lange-Nielsen syndrome, which is caused by homozygous loss-of-function mutations of *KVLQT1* or *KCNE1* potassium channel genes (Neyroud et al., 1997; Schulze-Bahr et al., 1997; Splawski et al., 1997a; Tyson et al., 1997). Consistent with this thesis, all parents were unaffected, and one of the families had two children with TS. However, none of the parents from any family were related, and consanguinity would be expected in a rare recessive syndrome. By contrast, the complexity of the TS phenotype suggested a second possibility, a contiguous gene deletion syndrome or a chromosomal rearrangement. Karyotypic analysis of metaphase chromosomes from 11 children failed to reveal defects (data not shown). This analysis, however, would not exclude small deletions.

A consistent feature of TS was severe QT interval prolongation. Therefore, to define the genetic basis of this disorder, we screened known long QT syndrome genes, including *HERG, KVLQT1, KCNE1, KCNE2*, *SCN5A*, and *KCNJ2*, by single-strand conformation polymorphism (SSCP) and/or DNA sequence analyses. We also examined several other genes encoding channel or channel-associated subunits, including *FKBP1A*, *KCNA4*, *KCNA5*, *KCND3*, *KCNE3*, *KCNIP2*, *KCNJ4*, *KCNJ9*, *KCNJ10*, *KCNJ12*, *NCX1*, *SCN1B*, *DNAJB1*, and *TRPC3*. The transcription factors *TFAP2B*, *FOG2*, *NKX2.5*, and *GATA4* were tested because they have been implicated in one or more phenotypic features of TS. No mutations were identified.

The abnormal electrocardiographic morphology observed in TS patients was similar to that of individuals with long QT syndrome caused by gain-of-function mutations in SCN5A, the cardiac sodium channel (Zhang et al., 2000). The cardiac L-type calcium channel $Ca_V1.2$, like SCN5A, mediates an inward depolarizing current in cardiomyocytes. Thus, in 1996, we examined the $Ca_V1.2$ gene as a candidate. SSCP analyses of 47 exons and promoter regions did not show mutations (Table 2). However, new alternatively spliced forms of the $Ca_V1.2$ gene were subsequently identified (Abernethy and Soldatov, 2002). Analysis of one $Ca_V1.2$ splice variant revealed a G1216A transition in exon 8A in all 13 individuals for whom DNA samples were available (Figures 2A and 2B). This transition caused a substitution of glycine with arginine at residue 406 (G406R). This amino acid is completely conserved in other voltage-dependent calcium channels of multiple species, ranging from worms to humans (Figure 2C). G406 is located at the C-terminal end of the sixth transmembrane segment of domain I (DI/S6, Figure 2D). The G406R mutation was not identified in 180 ethnically matched control samples (360 chromosomes, $p = 1.8 \times 10^{-20}$).

Mutational analysis of additional family members, including parents, failed to reveal mutations at this site. Thus, the phenotype in all probands resulted from the same de novo mutation. However, in one family, two siblings had the syndrome (Figure 2B). Both parents were phenotypically unaffected. The probability of the mutation event happening twice in the same family was minimal. To explain this apparent paradox, we hypothesized that one parent was mosaic for the mutation. Mosaicism is defined by the presence of two or more genetically different cell types in the same organism. To test this hypothesis, we sequenced DNA samples from the father's sperm and blood, but the mutation was not observed. In the mother, we sequenced DNA samples from blood and oral mucosa. Although the blood DNA contained only wild-type sequences, we were able to detect a small peak for the missense mutation in DNA from the oral mucosa (Figure 2B). These findings indicate that the mother is mosaic and transmitted this mutation to her two affected children. To further test this hypothesis, we performed genotypic analysis in this

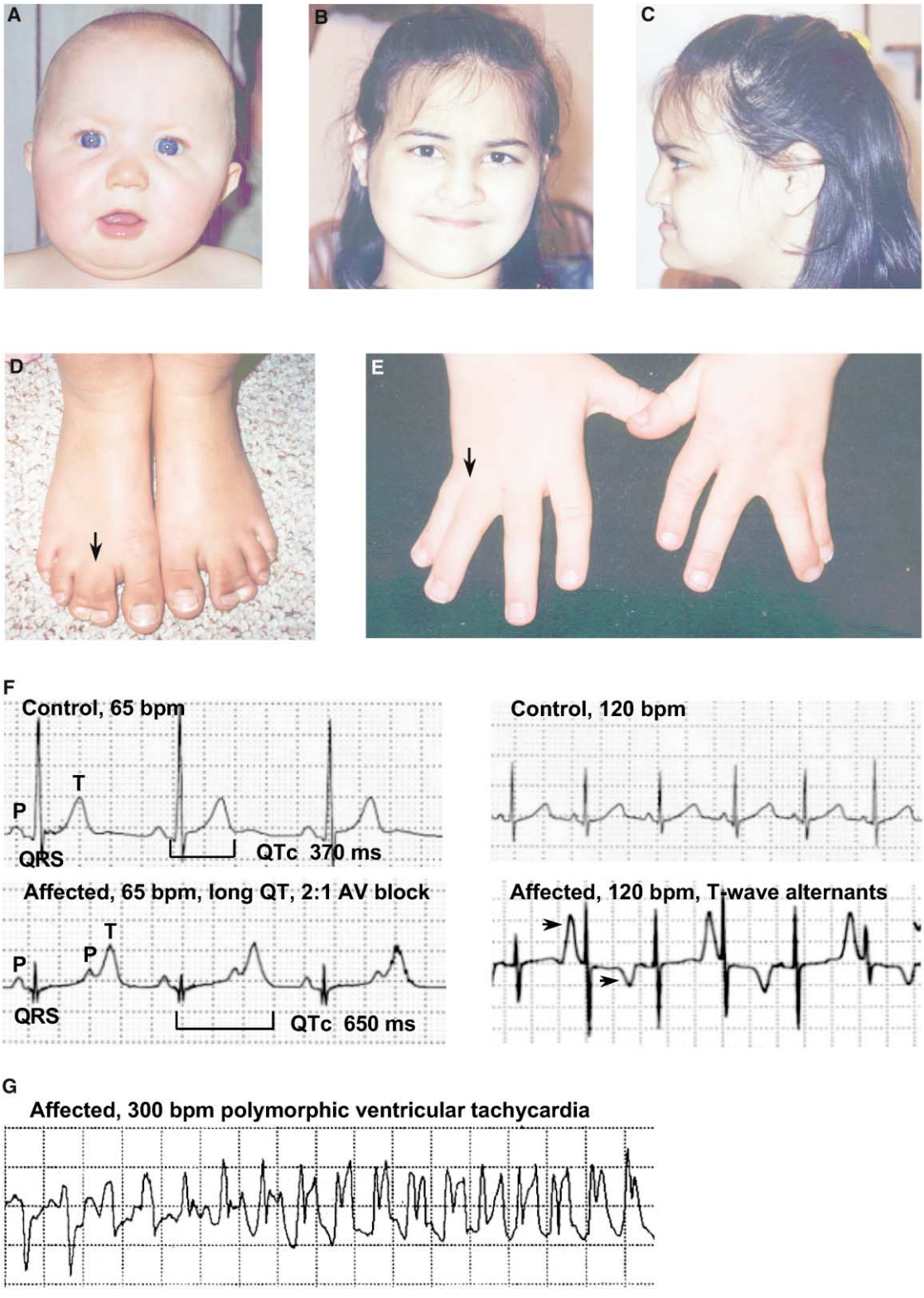

Figure 1. Timothy Syndrome Is Characterized by Multisystem Dysfunction and Developmental Defects

(A–C) TS individuals exhibiting dysmorphic facial features including round face, flat nasal bridge, receding upper jaw, and thin upper lip.

(D and E) Webbing of the toes and fingers (syndactyly).

(F) Left panel electrocardiogram shows severe QT interval prolongation causing 2:1 atrioventricular block seen as two atrial beats (P-waves) for each ventricular beat (QRS complex). Right panel electrocardiogram shows alternating T-wave polarity (arrows), indicating severe cardiac repolarization abnormality.

(G) Ventricular tachycardia recorded from a TS patient by an implanted automatic defibrillator.

Table 1. Phenotypic Features of Timothy Syndrome

Phenotype	Affected[a] (%)
Heart	
QT prolongation	100
Arrhythmia	
(1) Ventricular tachyarrhythmia	71
(2) Bradycardia, AV block[b]	94
Patent ductus arteriosus	59
Patent foramen ovale	29
Ventricular septal defects	18
Tetralogy of Fallot	6
Cardiomegaly	35
CNS	
Autism	60
Autism spectrum disorders	80
Mental retardation	25
Seizures	21
Umbilical cord	
Two vessel	13
Gastrointestinal	
Gag reflex	31
Skin	
Syndactyly	100
Bald at birth	100
Face	
Dysmorphia	53
Eyes	
Myopia	25
Nose	
Sinusitis	29
Teeth	
Small	100
Cavities	50
Lungs	
Pneumonia/bronchitis	47
Pulmonary hypertension	21
Hypothyroidism	8
Hypocalcemia	33
Hypoglycemia	36
Hypothermia	33
Muscoskeletal	
Hypotonia	40
Immunodeficiency/recurrent infections	43

[a] Nine affected individuals were male, and eight were female.
[b] Atrioventricular block.

family. We found that the G406R mutation resided on the maternal chromosome. Thus, in one case, G406R arose de novo in a parent during development, leading to mosaicism. Taken together, these data indicate that a recurrent, de novo G406R mutation of the $Ca_V1.2$ gene causes TS.

$Ca_v1.2$ Is Widely Expressed

Previous studies indicate that the $Ca_V1.2$ gene was expressed in heart, brain, smooth muscle, and pituitary and adrenal glands (Ertel et al., 2000). However, the TS phenotype suggested a broader expression pattern of the alternatively spliced form of $Ca_V1.2$ containing exon 8A. To determine the pattern of expression in humans, we used exon 8A as a probe for Northern and dot blot analyses (Figure 3). This exon was highly expressed in adult heart, and the mRNA was $\sim$9 kb (Figure 3A). mRNA containing exon 8A was also expressed in multiple adult and fetal tissues, including brain, gastrointestinal system, lungs, immune system, smooth muscle, and testis. These data indicate that exon 8A of the $Ca_V1.2$ gene is widely expressed in humans.

Exons 8 and 8A are mutually exclusive as they encode the same structural domain (DI/S6), but one must be present to encode a functional channel. To quantify the relative expression of exons 8 and 8A in human heart and brain, we cloned these exons from cDNAs. We found that 23 of 101 clones (22.8%) from heart cDNAs contained exon 8A, and 78 clones (77.2%) contained exon 8. In the brain, 13 of 56 clones (23.2%) contained exon 8A, and 43 clones (76.8%) contained exon 8. The relative expression of exon 8A is consistent in heart and brain and is expressed at significantly lower levels than exon 8.

To define the cellular distribution of $Ca_V1.2$ gene expression, we performed in situ hybridization experiments in mice. $Ca_V1.2$ was expressed throughout the brain (Figure 4A), including hippocampus, cerebellum, and amygdala. Abnormalities of these brain regions have been implicated in autism (Allen and Courchesne, 2003; Brambilla et al., 2003). $Ca_V1.2$ showed highest expression in the granular layers of hippocampal dentate gyrus (Figures 4A and 4B) and cerebellum (data not shown). $Ca_V1.2$ was also expressed throughout the heart (Figures 4C and 4D) and the vascular system, including ductus arteriosus (Figure 4E). In the eye, $Ca_V1.2$ was expressed in the retina and sclera (Figure 4F). $Ca_V1.2$ was also expressed in developing digits and teeth (Figures 4G and 4H). Thus, the expression pattern of $Ca_V1.2$ in humans and mice is consistent with the phenotypic abnormalities associated with TS.

G406R Mutation Impairs Channel Inactivation

To determine the molecular consequences of the G406R mutation, we heterologously expressed wild-type (wt) and mutant (G406R) forms of the $Ca_V1.2$ channel in Chinese hamster ovary (CHO) cells and *Xenopus* oocytes. The biophysical properties of the channel were first characterized by standard whole-cell patch-clamp techniques using Ca^{2+} (15 mM) as a charge carrier in CHO cells cotransfected with $Ca_V1.2$ and its accessory subunits, $Ca_V\beta_{2b}$ and $Ca_V\alpha_2\delta_1$. The most striking difference between wt and G406R channels was the extent of inactivation. Inactivation of wt channel current was nearly complete in 300 ms (Figure 5A). In contrast, G406R channels only partially inactivated during the same time period (Figure 5B). Next, we assessed the voltage dependence of Ca^{2+} current inactivation. Wild-type channel inactivation was complete at $+20$ mV and slightly decreased at more positive potentials, as expected for partial relief of the Ca^{2+}-dependent component of inactivation (Lee et al., 1985) (Figure 5C). In contrast, the maximum attained inactivation was only 56% for G406R channels. Relief of inactivation was greater for G406R compared to wt channels at potentials $>+30$ mV (Figure 5C). This observation suggests that mutant channels have lost voltage-dependent Ca^{2+}current inactivation. The time constant for inactivation (τ) was a U-shaped function of voltage for wt channels but increased with membrane voltage for mutant channels (Figure 5D). The current amplitudes measured at the peak of the current-voltage (I/V) relationship were similar ($p = 0.32$) and averaged 70 ± 12 pA for wt ($n = 11$) and 94 ± 20 pA for G406R ($n = 9$). The shape of the normalized I/V relationship (Figure 5E) was only slightly altered by the mutant channels, consistent with a mere -3 mV shift in

Table 2. Oligonucleotide Pairs Used to Amplify Exons of $Ca_V1.2$ Gene

Exon	Forward Oligonucelotide	Reverse Oligonucleotide	Size (C)[a]
1	TGAGCAGGATAATTATTTAGCTTT	TTCAACATGTTCTTCCTACTCTT	246 (1)
1A	ACATTTCTTCCTCTTCGTGGC	GCGGGTAGGGCAGGAACC	167 (2)
2[b]	TGCCCCTGTTTTCTATCTAGTA	CGCTGCGTGGAGCTGACTG	245 (2)
2[b]	ATGGGCAGCGCTGGCAATG	GCATGCCCAGCCCGGTGAA	208 (2)
3	GTACTTTCTGTGGCATTAACTTC	CGCAGTTCTCCATCGAGTGA	198 (1)
4	AATCCCCAAACCAATGACTTATT	GTCCCGCAACACTGGTAAGAT	243 (1)
5	GGGCAAAAGAAAACCCAGTCC	CTGTACACAAGAACGGGCTTC	219 (1)
6	TACCGCGGTGATGCTTGGTT	GGGCCTTGGGAGCGCAGC	237 (2)
7	CCCTGCTGCTCCCGTCTC	TGACTGCCCACTCATGCTAC	262 (2)
8	CTTCTTTCCTAACTTTCCTTCG	CTGCGTTGTGGAGAGGACATA	172 (1)
8A	GTGCCTCACTAACTATCATTCC	AAATCAAGACCTTTTTCCTTGGT	168 (2)
9	CCTGCCCCTCCTCTCACTC	CCCAAACACAGAAGAAGACGG	228 (2)
10	TCCCCACCCTCAATGCCTG	GAAAAAGCCCCAGCCCCTG	175 (2)
11	ATCAAATTTCCCTGGGACTGTT	AGGAAGGAAGAGCAGCGTGA	142 (1)
12	CAGCCAACCCCACCCTTCT	TACCAGGAGGAAACCAGAGCA	240 (2)
13	CTGGCCCTGCTCGGATCTC	AAGAACTTCTTCCTGAGTCCC	318 (1)
14	GGGCAGAGTGCTGACCTCC	ACCCCGAGTCCGAATCCCA	285 (1)
15	AACGCTGTGTCCCTTATTGGT	GGGGCAGCAGCAAAGGATAC	179 (1)
16	AACCAAGGGTCATTTTCTTTAAG	CAGGCCTGGGCAAGCTTAGA	180 (1)
17	TCACTCCAGTAAACAGCCATT	ACAGCTCCAGGAAGGAGACA	198 (1)
18	CCCCTTCTCCCCTGTGACT	CTCCCAATCCCAGGTTAGGC	129 (1)
19	AGTGGGAGTGCTGGAGTTATT	TGCCAGGCTGGTACTAGAGAG	235 (2)
20	TCTCTCCTCCTGTCCCCTCT	TGCAGAAGACACAGGCGATG	184 (2)
21	CATCCCATCCCCACCCTGTT	TGCTGGCACAAGGGGGACA	144 (2)
22	ACTCTCAGAGCCACTAATCCAA	GAGATAGACAAAGAAAGCGACA	148 (1)
23	GGCCACTCACACTGGTGTTC	AGCTGCATGGCCCATCGTG	185 (1)
24	CCAGAAACAGGAGGAGCTTAC	CTGGAGACTCCCTACCCAAG	166 (1)
25	ATCTCCTGAAGCCACGTCCC	AGGTAGGAGGACCACAACGG	186 (2)
26	TTGCTTTTGGATTGACTCATTGA	GCCCTCCCACCTCTACTCA	135 (1)
27	GATCCCAGAGTAAACTCCTTC	GTGGGGCCTTGCTTTGCATA	207 (1)
28	ACCCTGCTTCTCCAGTTCC	CCGCTTCCCTCCGCTCCTT	280 (2)
29	AGCGACAGTGCGTGGAATAC	TGCTCCTCCTGGGACTGAC	182 (1)
30	CACAGCTCCTCCCCTCTCC	CTGATGCCTGGGAATCAAAGG	177 (1)
31	TTCCTTTTTAATCCCCATCCTG	TCCTGGGGAGGGCAGAGTAA	152 (2)
32	TTTGTCCTTTCTTGTTGGTTCTT	AGCAGGCACGGACGGTTAG	182 (2)
33	TACCGGGCATCTTCATGGGA	AGAGTGGGGGTGTTAGAGGG	154 (1)
34	GCACCTCCTGTTGCCGACG	GGCCGCAGGACATGAGGG	182 (2)
35	CTGCACTCCAGCCTCATGG	GCCCCGTGGTGGGAGCCT	132 (2)
36	GGGCTGCATGAACGTGGCT	ATGGCTGCTGGCTGTTGAGT	235 (2)
37	GGATGGGCTGCATGAACGTG	ATGGCTGCTGGCTGTTGAGTT	239 (1)
38	GAAGGTCTTCTCACAGCACC	CTCAGCTTGGGGAATCAGGA	210 (2)
39	CTCTCTGATGCCCTGTCCCT	CTCTCCCTCCCATGAACCC	168 (2)
40	GCACCGCCTGCCATCATCA	GTCTCTCCCAGTGCCCACG	178 (1)
41	CACCATCTGTGGCTTCCTAC	GCGGGAGTCCAGGGAGCA	211 (2)
42	CCCTGCTCCCCTCTTACCC	GGCAATGACCAGGACCTTCC	222 (1)
43	GAGGAAAGGGAGCGTGGTC	CTTTATAGGGGTCGAGAGTGC	218 (1)
44[b]	TGGGTGCTAAGGGGCTTCTC	CGTTGTTGATGTTGGCGTTGG	263 (2)
44[b]	CTCCACCTTCACCCCGAGC	TGCAGCACGTGGGCCCTGT	246 (2)
45	TCTCCTTGTCCTCTCATCCC	CTGGAGGGCGAGCATGTCAA	267 (1)
45A	GCCTTGGTCCAGAGCTAAAG	CTGGCACCCTGGGGTAAAG	187 (2)
46	GGAAGGTTGGCAGTTTCTGAT	CAGCCTCAGCAGAGGGCAG	205 (1)
47[c]	GGGGTGCAGCTGTCCCTGT	CCGCCGACCACATCCAGAG	216 (2)
48	CTGTTTTCCTGCCCTGATGGT	GTGGCCTGTCCAAAAGTGTGA	173 (1)
49[b]	CGGCCACTCCTATTAACTCAC	AGGAGCCGCAGTGGATGGAT	239 (2)
49[b]	TTGAGGGGGTCGAGTCCAG	CCTGCCCATCTGCGAGTCA	221 (2)
50[b]	GTTCCTTTGGTTCTTCATGGCT	CCTGCAGTTCACAAAGGGTAA	226 (1)
50[b]	GCCGACAACATCCTCAGCG	AACCCATTAGGAACATTGAAACA	241 (1)

[a] (C), condition; two different conditions were used for PCR, see Experimental Procedures.
[b] Exons 2, 44, 49, and 50 are long, and each was amplified with two overlapping oligonucleotide pairs.
[c] Oligonucleotides for exon 47 also amplify an apparent noncoding duplication of the genomic sequences encompassing exons 45–49 found 3′ of the $Ca_V1.2$ gene. The duplicated exon 47 differs at several nucleotide positions, which should not be mistaken for mutations.

the voltage dependence of activation (Figure 5F). These data indicate that G406R substantially impairs voltage-dependent channel inactivation.

To confirm that the effect of the mutation was primarily a loss of voltage-dependent inactivation, we recorded wt and mutant channel activity in *Xenopus* oocytes using Ba^{2+} (40 mM) as a charge carrier. Ba^{2+} currents inactivate much slower than Ca^{2+} currents because, in the absence of extracellular Ca^{2+}, channel inactivation is almost entirely dependent on transmembrane voltage (Lee et al., 1985). The time-dependent inactivation was dramatically reduced by the mutation (Figures 5G and

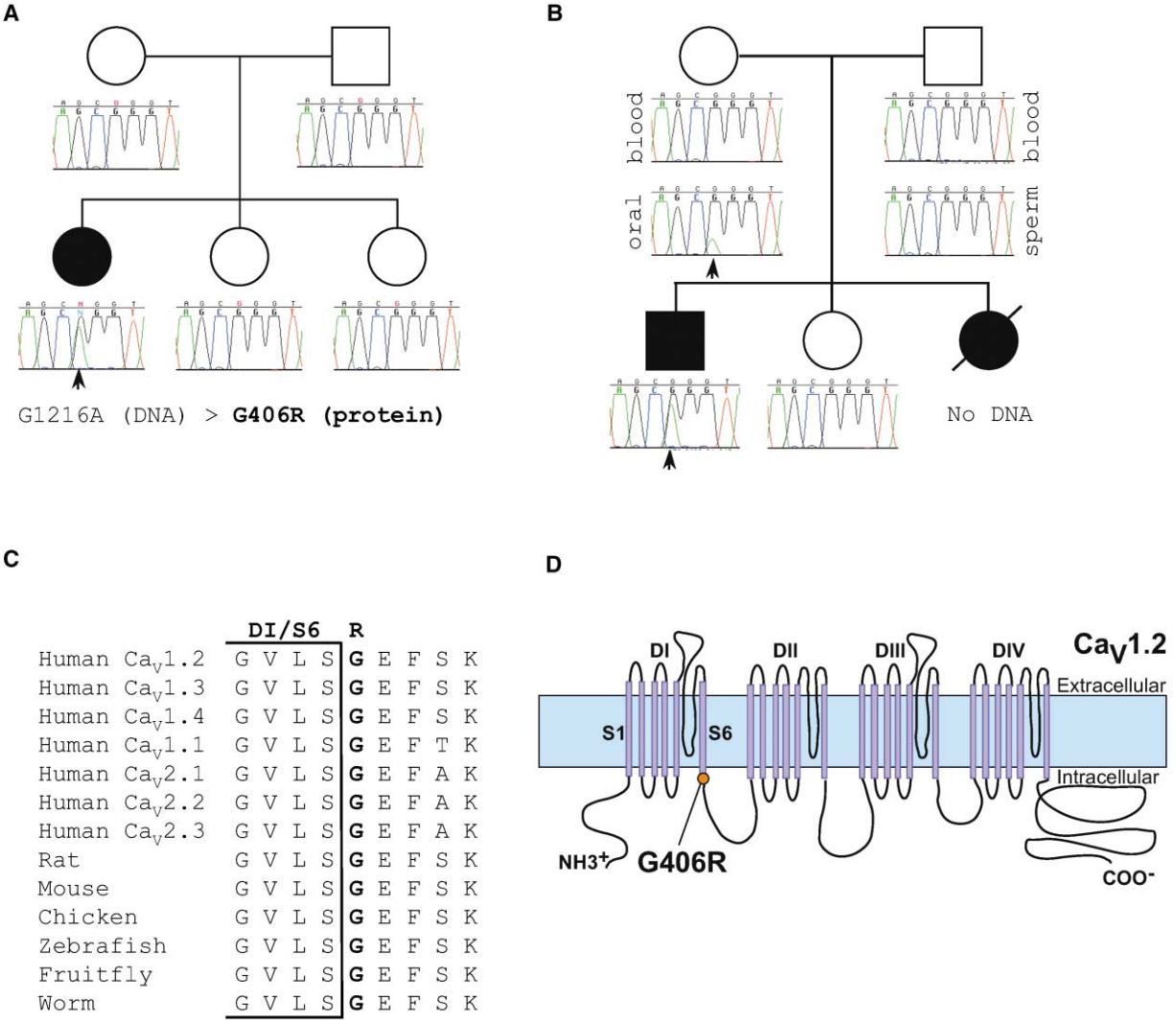

Figure 2. Identical De Novo $Ca_v1.2$ Missense Mutation Causes Timothy Syndrome

(A) TS pedigree showing sporadic occurrence of the disease phenotype and de novo G1216A missense mutation. This mutation leads to the substitution of glycine 406 with arginine (G406R). Circles and squares indicate females and males, respectively. Filled and empty symbols denote affected and unaffected individuals. Sequence tracings were derived from blood DNA samples unless otherwise indicated.

(B) TS family with two affected children. A small mutant peak (green, arrow) in the mother's sequence from oral mucosa DNA is apparent. This peak is not seen in the sequence of her blood DNA, indicating mosaicism. Germline mosaicism explains the presence of two affected children in this family. The individual with a slash is deceased.

(C) Amino acid sequence alignment showing conservation of glycine 406 from multiple species. Bracket indicates the end of the sixth transmembrane segment of domain I (DI/S6).

(D) Predicted topology of $Ca_v1.2$, showing the location of the mutation.

5H). Next, we determined the voltage dependence of inactivation. Whereas wt channels inactivated >90% after a conditioning pulse to +30 mV, G406R channels inactivated <20% at the same potential (Figure 5I). These data demonstrate that the G406R mutation produces maintained inward Ca^{2+} currents by causing nearly complete loss of voltage-dependent $Ca_v1.2$ channel inactivation.

Block of L-type calcium channels by dihydropyridines is enhanced by inactivation (Bean, 1984; Sanguinetti and Kass, 1984). To determine if mutant channels with defective inactivation were still affected by these drugs, we measured nisoldipine block of Ba^{2+} currents in *Xenopus* oocytes. The IC_{50} (the drug concentration at which 50% of the current is inhibited) for block of peak current by nisoldipine was 74 ± 7 nM for wt channels (two to six cells per concentration). The IC_{50} for G406R channels was 267 ± 5 nM for peak currents and 136 ± 11 nM (three to seven cells per concentration) for current measured at the end of a 1 s pulse. These data indicate that mutant channels remain sensitive to dihydropyridines and suggest that these drugs or other calcium channel blockers may be useful to treat TS.

G406R Prolongs Simulated Action Potentials

A prominent feature of TS is prolongation of the QT interval and lethal arrhythmias. An important function of $Ca_v1.2$ channels is mediating the plateau phase of the

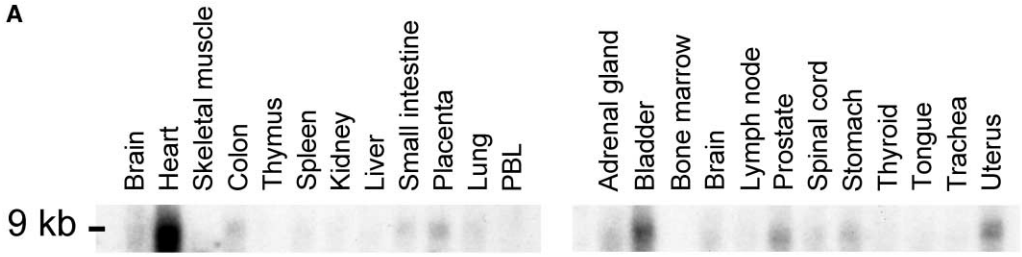

B

	1	2	3	4	5	6	7	8	9	10	11
A	whole brain	cerebellum, left	substantia nigra	heart	esophagus	colon, transverse	kidney	lung	liver	leukemia, HL-60	fetal brain
B	cerebral cortex	cerebellum, right	accumbens nucleus	aorta	stomach	colon, descending	skeletal muscle	placenta	pancreas	HeLa S3	fetal heart
C	frontal lobe	corpus callosum	thalamus	atrium, left	duodendum	rectum	spleen	bladder	adrenal gland	leukemia, K-562	fetal kidney
D	pareital lobe	amygdala	pituitary gland	atrium, right	jejunum		thymus	uterus	thyroid gland	leukemia, MOLT-4	fetal liver
E	occipital lobe	caudate nucleus	spinal cord	ventricle, left	ileum		peripheral leukocyte	prostate	salivary gland	Burkitt's lymphoma Raji	fetal spleen
F	temporal lobe	hippo-campus		ventricle, right	ilocecum		lymph node	testis	mammary gland	Burkitt's lymphoma Daudi	fetal thymus
G	postcentral gyrus	medulla oblongata		interventr. septum	appendix			ovary		colorectal carcinoma	fetal lung
H	pons	putamen		apex of the heart	colon, ascending		trachea			lung carcinoma	

Figure 3. The $Ca_v1.2$ Gene Is Widely Expressed

(A) Human Northern blot analyses show expression of $Ca_v1.2$ mRNA containing exon 8A in brain, heart, bladder, prostate, uterus, stomach, and other tissues.

(B) mRNA dot blot demonstrates expression of $Ca_v1.2$ mRNA containing exon 8A in multiple tissues, including many regions of the brain.

cardiac action potential. We predicted that a slowed rate of channel inactivation would prolong the inward (depolarizing) Ca^{2+} current during the plateau phase and delay cardiomyocyte repolarization. We determined that, in the heart, 23% of $Ca_v1.2$ channels contained exon 8A. Thus, in the heterozygous state, only 11.5% of $Ca_v1.2$ channels carry the G406R mutation. To simulate the effect of the TS mutation, we assumed these ratios in a dynamic model of a mammalian ventricular myocyte (Faber and Rudy, 2000). We altered the voltage dependence of L-type calcium channel inactivation to mimic the expected biophysical effects of the mutation in heterozygous condition (Figure 6A, blue triangles). The net effect on total $Ca_v1.2$ channel inactivation was small. However, this resulted in a maintained inward Ca^{2+} current that prolonged action potential duration by 17% (Figure 6B, blue traces). Simulations also indicated that 35% reduction of the abnormal L-type Ca^{2+} current could restore normal action potential duration (Figure 6B, red traces). These data indicate that G406R mutation causes substantial prolongation of cardiac action potentials, consistent with the QT interval prolongation and increased risk of arrhythmia in TS.

Discussion

We conclude that the G406R mutation of the $Ca_v1.2$ L-type calcium channel causes the diverse physiological and developmental defects in TS. Several lines of evidence support this conclusion. First, we identified an

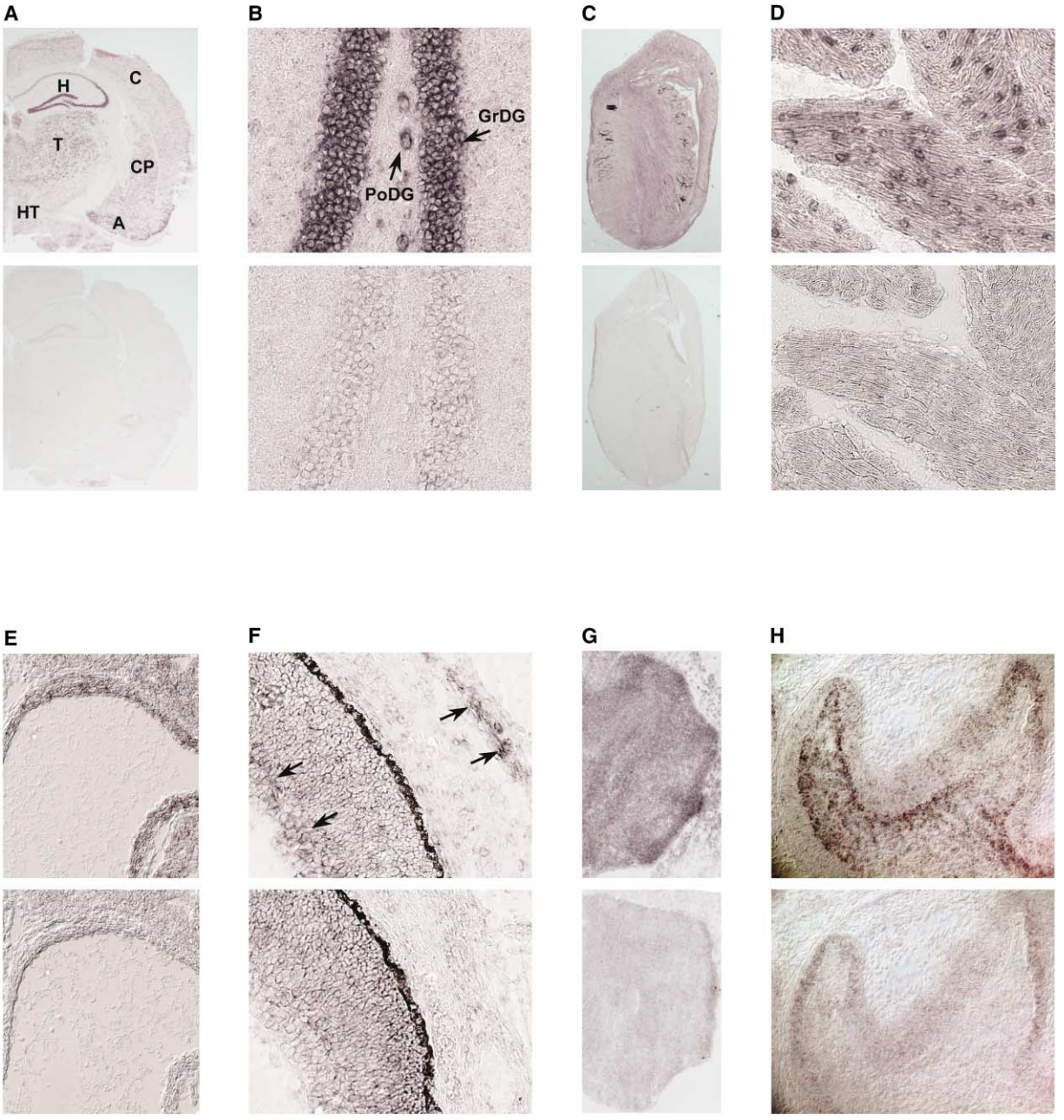

Figure 4. The $Ca_v1.2$ Gene Is Expressed in Multiple Mouse Tissues

(A) In the brain, the $Ca_V1.2$ gene is expressed in cortex (C), hippocampus (H), thalamus (T), hypothalamus (HT), caudate putamen (CP), and amygdala (A). For all tissues, in situ hybridization experiment with antisense probe is shown in the top panel, and sense probe (control) is shown beneath.

(B) Magnification shows expression in the granular (GrDG) and polymorph (PoDG) layers of the hippocampal dentate gyrus.

(C) $Ca_V1.2$ gene is expressed throughout adult heart.

(D) Higher magnification of heart ventricle.

(E–H) Expression in ductus arteriosus ([E], E12.5), retina (left arrows), and sclera (right arrows) of eye ([F], E16.5), developing digits ([G], E12.5), and tooth papilla ([H], P0).

identical, de novo missense mutation of the $Ca_V1.2$ gene in 13 of 13 TS individuals. This mutation was not present in controls, and the affected amino acid G406 was completely conserved across species. Second, expression of the $Ca_V1.2$ gene in brain, teeth, digits, lungs, ductus arteriosus, and the immune system was consistent with the TS phenotype. Third, the $Ca_V1.2$ gene was strongly expressed in the heart. Gain-of-function mutations of this gene would be expected to cause long QT syndrome and cardiac arrhythmias. Fourth, functional expression of mutant channels demonstrated that G406R had a dramatic effect on channel inactivation, causing pro-

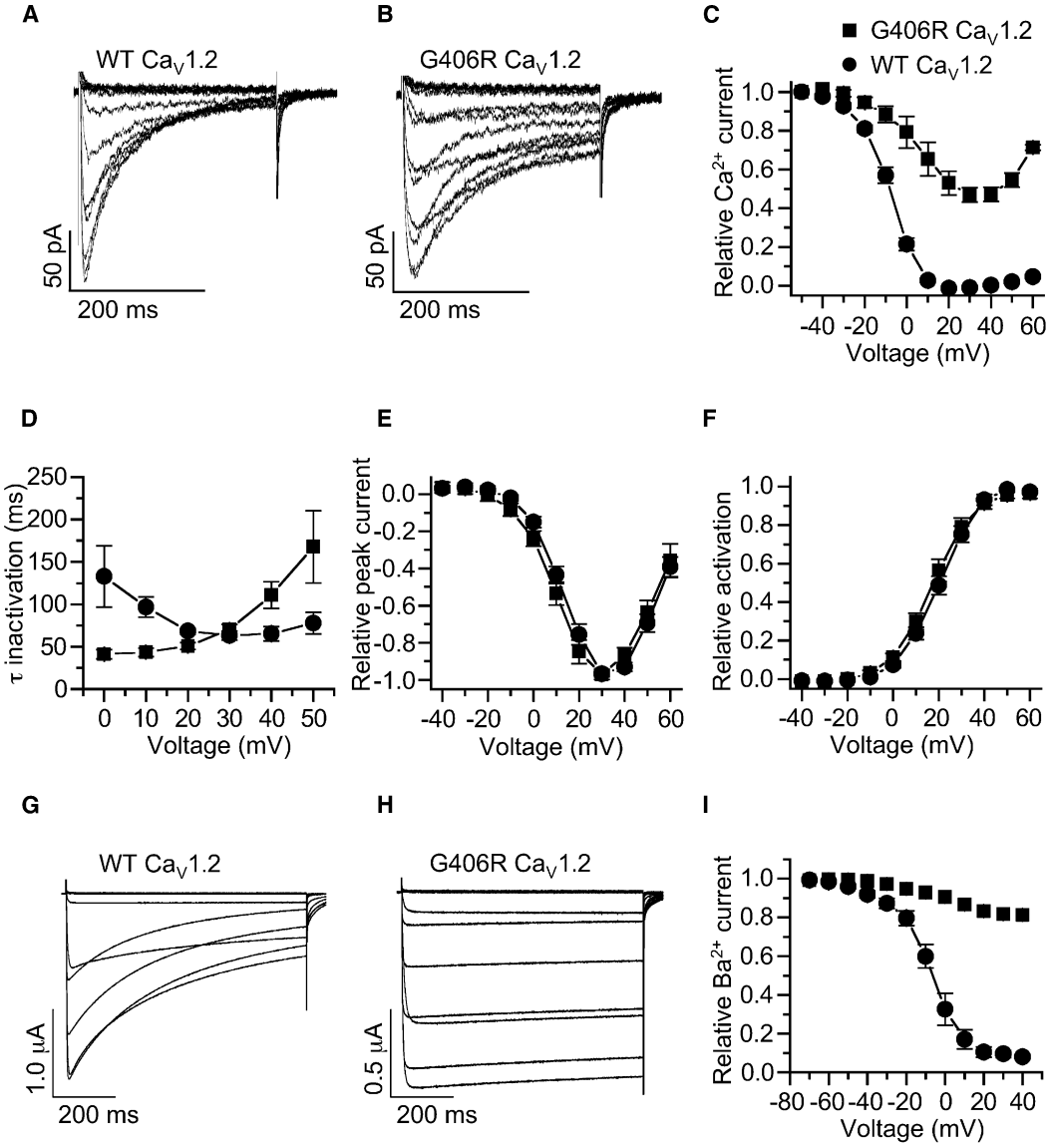

Figure 5. Timothy Syndrome Mutation Reduces $Ca_v1.2$ Channel Inactivation

Inactivation is a time-, voltage-, and Ca^{2+}-dependent decrease of channel current. (A and B) Wild-type (A) and G406R (B) $Ca_V1.2$ channel currents recorded from CHO cells in response to voltage pulses applied in 10 mV increments from −40 to +60 mV. External solution contained 15 mM $CaCl_2$. Note that inward Ca^{2+} current is markedly prolonged by the mutation. (C) Voltage dependence of Ca^{2+} current inactivation in CHO cells for wt channels (circles; $V_{1/2} = -8$ mV, k = 6.9 mV; n = 5) and G406R channels (squares; $V_{1/2} = 4$ mV, k = 10.6 mV; n = 5). Note that the overall extent of G406R channel inactivation is reduced and that the Ca^{2+}-dependent component of inactivation (ascending limb of the relationship) is accentuated. These data suggest reduced voltage-dependent inactivation for G406R channels. Reduced inactivation results in a maintained inward current and delayed repolarization of the action potential.

(D) Time constants of Ca^{2+} current inactivation as a function of voltage (n = 5–9).

(E) G406R channels have similar Ca^{2+} current-voltage (I/V) relationship compared to wt.

(F) Voltage dependence of Ca^{2+} current activation is not significantly altered by the mutation (n = 9–11).

(G and H) G406R causes nearly complete loss of voltage-dependent channel inactivation. Wild-type (G) and G406R (H) $Ca_V1.2$ channel currents were recorded from *Xenopus* oocytes in response to voltage pulses applied in 10 mV increments from −70 to +40 mV. External solution contained 40 mM $BaCl_2$ to eliminate Ca^{2+}-dependent inactivation.

(I) Voltage dependence of Ba^{2+} current inactivation in oocytes for wt ($V_{1/2} = -8$ mV, k = 8.9 mV; n = 7) and G406R channels ($V_{1/2} = 0$ mV, k = 15.9 mV; n = 6).

longed inward Ca^{2+} currents. Finally, simulation analysis indicated that the G406R effect on channel function causes significant action potential prolongation, consistent with the TS phenotype.

It is remarkable that all TS individuals carry the identical de novo mutation. One reason that G406R always arose de novo is the early fatality caused by the mutation, making its inheritance rare. Two factors may explain the unusual recurrence of this mutation. First, our physiological studies indicate that arginine at this posi-

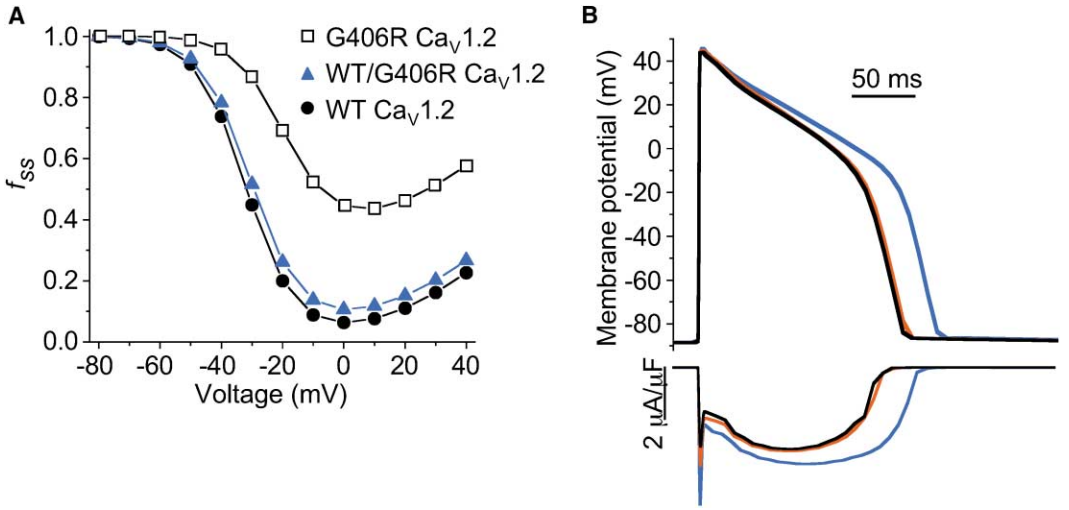

Figure 6. Computer Modeling Shows Prolonged Action Potentials in G406R Heterozygotes

(A) Simulated voltage dependence of calcium channel current inactivation for wt (circles), G406R (squares), and wt/G406R heterozygotes (blue triangles). The relative voltage-dependent inactivation gate term f_{ss} is plotted as a function of transmembrane voltage. In the heart and brain, mRNA analysis indicated that ~23% of $Ca_V1.2$ channels contain exon 8A. As a result, heterozygotes are predicted to express 11.5% mutant channels, leading to small effect on total $Ca_V1.2$ channel inactivation.

(B) Although the net effect on total $Ca_V1.2$ channel inactivation is small, cardiac action potentials (upper panel) are prolonged by 17%. L-type Ca^{2+} currents for wt (black) and heterozygous (blue) channels are shown in the lower panel. Hetrozygous Ca^{2+} currents must be reduced by 35% to simulate normal action potentials (red trace).

tion has a profound gain-of-function effect. Gain-of-function mutations are uncommon and may be domain specific. The DI/S6 segment is known to be important for voltage-dependent inactivation of calcium channels (Herlitze et al., 1997; Shi and Soldatov, 2002; Zhang et al., 1994). Second, the mutated nucleotide (G1216) is located in a CpG dinucleotide on the noncoding strand. Deamination of a methylated cytosine causes the mutation of CpG to TpG, the most common mechanism for mutations (Cooper and Youssoufian, 1988; Vitkup et al., 2003). Transition from C to T would result in the observed G to A change on the coding strand in a subsequent cycle of DNA replication. Thus, this is a mutational hotspot. Together, these factors explain the unusual recurrence of G406R.

How does a single amino acid substitution of $Ca_V1.2$ cause the striking phenotypic abnormalities of TS? Explanations include the great impact of G406R on channel function and the wide tissue expression of $Ca_V1.2$. In the pancreas, Ca^{2+} mediates insulin secretion by pancreatic β cells. Episodic dysfunction of $Ca_V1.2$ signaling likely accounts for the intermittent hypoglycemia that led to the death of two affected children. In the heart, maintained depolarizing Ca^{2+} current through mutant $Ca_V1.2$ channels causes lengthening of cardiac action potentials. This, in turn, leads to QT interval prolongation and life-threatening arrhythmias. Now that we know the molecular basis of TS, prenatal and neonatal diagnosis is feasible. Early diagnosis is important, as cardiac arrhythmias and other features of this disorder are treatable.

By contrast with these physiological defects, many phenotypic abnormalities of TS, such as syndactyly and congenital heart disease, are developmental. $Ca_V1.2$ is highly expressed in apical ectodermal ridge cells of developing digits. It has been shown that destruction of these cells causes syndactyly (Hurle and Ganan, 1986). It is likely that Ca^{2+}-induced cell death (Orrenius et al., 2003) in the apical ectodermal ridge is the mechanism of syndactyly in TS. Abnormalities in cell death may also lead to the failure of the developing ductus arteriosus to properly close (Imamura et al., 2000; Tananari et al., 2000). Thus, TS demonstrates the importance of Ca^{2+} signaling in human development. Genetically modified mice harboring G406R may address mechanistic questions raised by these findings.

The fact that $Ca_V1.2$ is associated with autism is of great interest. The cardinal features of autism are severe difficulties in social interaction, communication deficits, and repetitive or ritualistic behavior. The severity of phenotypes varies considerably in autism spectrum disorders (ASD), which include autism, Asperger's syndrome, childhood disintegrative disorder, Rett syndrome, and pervasive developmental disorder not otherwise specified (PDD NOS). In the general population, autism spectrum disorders affect ~0.5% of children and cause great morbidity (Bryson et al., 2003; Volkmar and Pauls, 2003). Epidemiologic studies estimate that 200,000–400,000 children are affected in the United States alone (Fombonne, 2003). Despite their importance, very little is known about the molecular mechanisms of autism spectrum disorders (Zoghbi, 2003). Our findings that individuals with TS met the criteria for autism or had severe deficits of language and social development suggest that abnormal Ca^{2+} signaling may contribute to these disorders. As autism is a uniquely human phenotype, future work will focus on the genetic analysis of $Ca_V1.2$ and other calcium channels in nonsyndromic forms of autism and autism spectrum disorders. Future studies will also determine if features of TS are amenable to calcium channel blocker therapy.

Experimental Procedures

Subject Ascertainment and Phenotypic Analysis

Informed consent or assent was obtained from all individuals or their guardians according to standards established by local institutional review boards. Phenotypic analyses included history, physical examination, electrocardiography, and echocardiography. Five children were evaluated for behavioral phenotypes and cognitive development. These tests included the Diagnostic Criteria for Autistic Disorder, DSM-IV, Autism Screening Questionnaire, Autism Diagnostic Interview—Revised, the Child Behavior Checklist, Vineland Adaptive Behavior Scales, and the Autism Diagnostic Observation Schedule (Berument et al., 1999; Lord et al., 1994, 2000; Task Force on DSM-IV, 2000). Cognitive and language tests included Differential Ability Scales, Clinical Evaluation of Language Fundamentals—III, Goldman-Fristoe Test of Articulation, and NEPSY (Korkman et al., 1998).

Statistical Analysis

Fisher's exact test and data from the study with highest prevalence of autism and autism spectrum disorders (60 of 8,896 individuals) were used to determine the p value for the association of these disorders and TS (Bertrand et al., 2001). This comparison gave the most conservative estimate of the p value. Fisher's exact test was also used to assess the p value for the association of G406R with the TS phenotype.

Genotypic and Sequence Analyses

Genomic DNA from peripheral blood lymphocytes or cell lines derived from Epstein-Barr virus-transformed lymphocytes was prepared using Puregene DNA isolation kit (Gentra Systems). Genomic DNA from buccal swabs and sperm was prepared using QIAamp DNA Mini Kit (Qiagen). Oligonucleotides to all known exons of the $Ca_V1.2$ gene were designed to genomic sequences found in the Celera database using Oligo6.6 (Molecular Biology Insights, Table 2). PCR amplification of DNA samples and mutational analyses were carried out as previously described (Splawski et al., 1997b). Two different conditions were used for PCR: (1) 94°C for 2 min, 35 cycles of 10 s at 94°C, 20 s at 58°C, and 20 s at 72°C, followed by 5 min extension at 72°C; and (2) same as (1), but annealing was done at 54°C, and the PCR reaction had a final concentration of 10% glycerol and 4% formamide (Table 2).

Oligonucleotides OriF5′-TACACTAATCATCATAGGGTCAT and Ori2R5′-TAGCGATTCCCAGTTTAGGTAC were used to amplify a fragment of 1122 nucleotides containing part of exon 8A and adjacent intron 8A sequences. PCR products were obtained with Pfu Ultra HF DNA polymerase (Stratagene), purified, and sequenced. An intronic polymorphism (C to G) was identified 344 nucleotides downstream from exon 8A. PCR fragments were then cloned using the PCR-Script Amp Cloning Kit (Stratagene) to separate the products derived from individual chromosomes. DNA from several clones for each individual was sequenced to determine the parent chromosome on which the mutation arose.

mRNA Expression and cDNA Analyses

Blot analyses were performed using human 12-lane multiple-tissue Northern blots I and III (BD Biosciences Clontech). mRNA dot blot analysis was performed using the Multiple Tissue Expression Human Array 3 (BD Biosciences Clontech). A 115 base pair PCR fragment, amplified using HF5′-TGGGTCAATGATGCCGTAGG and HR5′-GAAAACTCTCCGCTAAGCACA oligonucleotides, was used as a probe for exon 8A containing mRNAs. The fragment was labeled with the Prime-It II labeling kit (Stratagene) using the reverse (HR) oligonucleotide instead of the provided random 9-mers. Hybridization and washing conditions followed manufacturer's suggestions. The blots were exposed to film for 3 days.

Human heart marathon-ready cDNA (BD Biosciences Clontech) and human heart and brain race-ready cDNAs (Ambion) were analyzed to estimate the ratio of $Ca_V1.2$ transcripts containing exon 8A to transcripts containing exon 8. Briefly, PCR products amplified using the 7F and 9R oligonucleotides (forward from exon 7, 7F5′-TCACGGTGTTCCAGTGCATC and reverse from exon 9, 9R5′-CAGGTAGCCTTTGAGATCCTC) were ligated into pGEM-T Easy Vector (Promega). Transformed colonies were screened by PCR for the presence of exons 8 or 8A using the original oligonucleotide pair. To identify colonies carrying only exon 8A, the same colony collection was then tested using a forward oligonucleotide specific to exon 8A (8AF5′-CTGGGTCAATGATGCCGTAG) and the 9R reverse oligonucleotide. DNA from 30 of 157 clones was sequenced to confirm the results. To control for the cloning efficiency of the fragments carrying each exon, we cloned PCR fragments amplified from a template mixture of cDNA containing exon 8 and cDNA containing 8A in a 1:1 ratio and screened colonies as detailed above. No difference in cloning efficiency was observed.

Nonradioactive in situ hybridization was performed as described (Berger and Hediger, 2001), using a digoxigenin (DIG)-labeled ~800 nucleotide cRNA probe from the C-terminal region of the mouse $Ca_V1.2$ gene. The probe was derived from a PCR fragment amplified from mouse heart Marathon-Ready cDNA (BD Biosciences Clontech) using MF5′-AGGCTGGCTTGCGCACCTT and MR5′-GAGAGATGTCTCCCCCTTGA oligonucleotides. Frozen sections (10 μm) were cut in a cryostat and captured onto Superfrost Plus microscope slides (Fisher). Sections were then fixed, acetylated, and hybridized to the probe (approximate concentration 100 ng/ml) over three nights at 70°C. Hybridized probe was visualized using alkaline phosphatase-conjugated anti-DIG Fab fragments (Roche) and 5-bromo-4-chloro-3-indolyl-phosphate/nitro-blue tetrazolium (BCIP/NBT) substrate (Kierkegard and Perry Laboratories). Sections were rinsed several times in 100 mM Tris, 150 mM NaCl, and 20 mM EDTA (pH 9.5) and coverslipped with glycerol gelatin (Sigma). Control sections were incubated with identical concentration of the sense probe transcript. Digital images for antisense and sense probes for each section were captured using identical microscope settings.

DNA Constructs for Functional Expression

Full-length human wt $Ca_V1.2$ cDNAs (accession number Z34815), cloned in a *Xenopus* (pBluescript) and mammalian (pcDNA3) expression vector systems, were a generous gift from Dr. N. Soldatov. The G406R mutation was introduced by site-directed mutagenesis using QuikChange (Stratagene) into the *Xenopus* expression clone. Subsequently, an AfeI/SgrAI fragment containing the introduced mutation was cloned into the AfeI and SgrAI sites of the wt pcDNA3 clone to obtain the mammalian G406R expression construct.

$Ca_V\beta_{2b}$ is the β subunit splice variant associated with $Ca_V1.2$ in the human heart (Colecraft et al., 2002). We obtained a cDNA clone containing the 5′ end sequence of $Ca_V\beta_{2b}$ from RZPD (clone DKFZp313F1242, RZPD, Germany) and purchased the splice variant $Ca_V\beta_{2a}$ (the 3′ sequences of $Ca_V\beta_{2a}$ and $Ca_V\beta_{2b}$ are identical) from Genecopoeia (clone GC-T4617, Genecopoeia). EcoRI/PshAI fragment from DKFZp313F1242 and PshAI/NotI fragment from GC-T4617 were cloned into the EcoRI and NotI sites of pcDNA3.1 (Invitrogen) to obtain the full-length cDNA clone for human $Ca_V\beta_{2b}$ (accession number AAG01473). The rabbit $Ca_V\beta_{2b}$ clone (accession number CAA45575, amino acid sequence 96% identical to human $Ca_V\beta_{2b}$) for expression in *Xenopus* oocytes was a kind gift from Dr. N. Dascal.

$Ca_V\alpha_2\delta_1$ is the $\alpha_2\delta$ subunit associated with $Ca_V1.2$ in the heart (Arikkath and Campbell, 2003). Full-length clone for the human $Ca_V\alpha_2\delta_1$ subunit (accession number NP_000713) was obtained by ligation of a NotI/Bpu10I fragment from IMAGE clone 2006073 and a Bpu10I/XbaI fragment from a PCR product, amplified from human heart Marathon-Ready cDNA (BD Biosciences Clontech) using oligonucleotides A2D1F5′-TGAATGTAGCTTCATTTAACAGCA-3′ and A2D1XbaR5′-GCTCTAGATTTGGCAGGGTCTGGAGTTTAAC-3′ (XbaI site underlined), into the NotI and XbaI sites of pcDNA3.1 (Invitrogen). The rabbit $Ca_V\alpha_2\delta_1$ clone (accession number AAA81562, amino acid sequence 96% identical to human $Ca_V\alpha_2\delta_1$) for expression in *Xenopus* oocytes was a kind gift from Dr. N. Dascal.

The full-length clones for all eight expression constructs described above were sequenced in forward and reverse direction and compared to genomic DNA to ensure that no unintended mutations were present or introduced.

Transfection and Solutions for CHO Cells

CHO cells were cultured in Ham's F-12 Media and transiently transfected using Lipofectamine 2000 (GIBCO). Cells were transfected

for 18 hr in 35 mm dishes containing 18 μl Lipofectamine, 242 μl Optimem (GIBCO), 0.86 μg enhanced green fluorescent protein (Molecular Probes), 4 μg of either wt or mutant human $Ca_V1.2$, and 1 μg each of human $Ca_V\beta_{2b}$ and human $Ca_V\alpha_2\delta_1$ subunit cDNAs. The extracellular solution contained the following, in mM: 130 NMDG, 15 $CaCl_2$, 5 KCl, and 10 HEPES (pH 7.4 with HCl, 22°C–25°C). The intracellular pipette solution contained the following, in mM: 120 Cs methanesulfonate, 5 $CaCl_2$, 2 $MgCl_2$, 10 EGTA, 2 MgATP, and 10 HEPES (pH 7.3 with CsOH). This solution results in an $[Ca^{2+}]_i$ of ~110 nM as calculated with WinMaxc (Bers et al., 1994).

Injection and Solutions for Oocytes

Isolation and injection of *Xenopus laevis* oocytes and synthesis of capped polyA cRNA from linearized cDNA templates were performed as described (Goldin, 1991). Oocytes were coinjected with cRNAs encoding wt or mutant human $Ca_V1.2$ subunit (11 ng) plus rabbit $Ca_V\beta_{2b}$ (2.7 ng) and rabbit $Ca_V\alpha_2\delta_1$ (2.7 ng) subunits. The extracellular solution contained the following, in mM: 40 $Ba(OH)_2$, 50 NaOH, 1 KOH, 5 HEPES (pH 7.4 with methanesulfonic acid, 22°C–25°C). Niflumic acid (300 μM) was added to the solution to block intracellular Ca^{2+}-activated Cl^- currents (White and Aylwin, 1990). Recording pipettes contained 3 M KCl and had resistances of 0.5–1 MΩ.

Voltage Clamp and Data Analysis

Whole-cell Ca^{2+} currents in fluorescent CHO cells were recorded using standard techniques (Hamill et al., 1981) and an Axopatch 200 patch-clamp amplifier (Axon Instruments) 2–3 days after transfection with cDNA. Voltage dependence of Ca^{2+} current inactivation in CHO cells was determined with a two-pulse protocol. The relative magnitude of inward current elicited during the second pulse (to +30 mV) was plotted as a function of the variable voltage of the first pulse (0.8 s). Ba^{2+} currents through calcium channels were recorded from oocytes using standard two microelectrode voltage clamp techniques (Stuhmer, 1992) 2–10 days after injection of cRNA. Voltage dependence of Ba^{2+} current inactivation in oocytes was determined with a two-pulse protocol. The relative magnitude of inward current elicited during the second pulse (to +10 mV) is plotted as a function of the variable voltage of the first pulse (2 s). Data acquisition and analyses were performed using pCLAMP8 (Axon Instruments). Currents were filtered at 2 kHz and digitized at 10 kHz. Data from CHO and *Xenopus* oocyte expression were fitted to a Boltzmann function to obtain half point ($V_{1/2}$) and slope factor (k) for the voltage dependence of $Ca_V1.2$ inactivation. Data are presented as mean ± SEM.

Action Potential Modeling

A dynamic model of mammalian ventricular myocytes (Faber and Rudy, 2000) was used to simulate the effect of the TS mutation in heterozygotes. For these simulations, the stimulation rate was set at 60 per min. Action potential waveforms and L-type Ca^{2+} currents were computed after 100 stimulations. Channel properties were modeled by altering the relative voltage-dependent inactivation gate term f_{ss} to a heterozygous condition in which the exon 8A containing $Ca_V1.2$ protein represents 23% (11.5% wt and 11.5% G406R) of the total $Ca_V1.2$ protein. Thus, the shifts in the inactivation curves caused by the G406R mutation (as measured in CHO cells) were reduced, assuming only 0.115 of the total channels were mutated ($V_{1/2}$ was shifted by +1.2 mV, and the minimal value for f_{ss} was set at 0.106).

Acknowledgments

We are grateful to all of the individuals with TS and their families for donated time and samples. We would also like to express our gratitude to C. Badame, K. Braegger, S. Etheridge, T. Carson, D. Goldman, T. Klitzner, J. Skinner, A. Moss, H. Stalker, G.M. Vincent, M. Marks, J. Towbin, M. Pun, C-L. Lien, GCRC Children's Hospital Boston, SADS Foundation, and the UK SADS Foundation. We thank N. Soldatov and N. Dascal for expression constructs and D. Clapham, S. Orkin, L. Kunkel, K. Thomas, and F. Engel for critically reviewing the manuscript. Funding from NIH (HL46401 and HL52338 for M.T.K. and M.C.S., DC03610 and MH66398 for H.T.-F.), Donald W. Reynolds Foundation (M.T.K. and I.S.), Fondazione Telethon, and Fondazione Cariplo (S.G.P.) is gratefully acknowledged.

Received: July 9, 2004
Revised: August 9, 2004
Accepted: August 17, 2004
Published: September 30, 2004

References

Abernethy, D.R., and Soldatov, N.M. (2002). Structure-functional diversity of human L-type Ca2+ channel: perspectives for new pharmacological targets. J. Pharmacol. Exp. Ther. *300*, 724–728.

Allen, G., and Courchesne, E. (2003). Differential effects of developmental cerebellar abnormality on cognitive and motor functions in the cerebellum: an fMRI study of autism. Am. J. Psychiatry *160*, 262–273.

Antzelevitch, C. (2003). Molecular genetics of arrhythmias and cardiovascular conditions associated with arrhythmias. J. Cardiovasc. Electrophysiol. *14*, 1259–1272.

APA (American Psychiatric Association) (2000). Diagnostic and Statistical Manual of Mental Disorders DSM-IV-TR, Fourth Edition (Washington, D.C.: American Psychiatric Association).

Arikkath, J., and Campbell, K.P. (2003). Auxiliary subunits: essential components of the voltage-gated calcium channel complex. Curr. Opin. Neurobiol. *13*, 298–307.

Bean, B.P. (1984). Nitrendipine block of cardiac calcium channels: high-affinity binding to the inactivated state. Proc. Natl. Acad. Sci. USA *81*, 6388–6392.

Bech-Hansen, N.T., Naylor, M.J., Maybaum, T.A., Pearce, W.G., Koop, B., Fishman, G.A., Mets, M., Musarella, M.A., and Boycott, K.M. (1998). Loss-of-function mutations in a calcium-channel alpha1-subunit gene in Xp11.23 cause incomplete X-linked congenital stationary night blindness. Nat. Genet. *19*, 264–267.

Berger, U.V., and Hediger, M.A. (2001). Differential distribution of the glutamate transporters GLT-1 and GLAST in tanycytes of the third ventricle. J. Comp. Neurol. *433*, 101–114.

Berridge, M.J., Bootman, M.D., and Roderick, H.L. (2003). Calcium signalling: dynamics, homeostasis and remodelling. Nat. Rev. Mol. Cell Biol. *4*, 517–529.

Bers, D.M., Patton, C.W., and Nuccitelli, R. (1994). A practical guide to the preparation of Ca2+ buffers. Methods Cell Biol. *40*, 3–29.

Bertrand, J., Mars, A., Boyle, C., Bove, F., Yeargin-Allsopp, M., and Decoufle, P. (2001). Prevalence of autism in a United States population: the Brick Township, New Jersey, investigation. Pediatrics *108*, 1155–1161.

Berument, S.K., Rutter, M., Lord, C., Pickles, A., and Bailey, A. (1999). Autism screening questionnaire: diagnostic validity. Br. J. Psychiatry *175*, 444–451.

Brambilla, P., Hardan, A., di Nemi, S.U., Perez, J., Soares, J.C., and Barale, F. (2003). Brain anatomy and development in autism: review of structural MRI studies. Brain Res. Bull. *61*, 557–569.

Brini, M., and Carafoli, E. (2000). Calcium signalling: a historical account, recent developments and future perspectives. Cell. Mol. Life Sci. *57*, 354–370.

Bryson, S.E., Rogers, S.J., and Fombonne, E. (2003). Autism spectrum disorders: early detection, intervention, education, and psychopharmacological management. Can. J. Psychiatry *48*, 506–516.

Catterall, W.A. (2000). Structure and regulation of voltage-gated Ca2+ channels. Annu. Rev. Cell Dev. Biol. *16*, 521–555.

Colecraft, H.M., Alseikhan, B., Takahashi, S.X., Chaudhuri, D., Mittman, S., Yegnasubramanian, V., Alvania, R.S., Johns, D.C., Marban, E., and Yue, D.T. (2002). Novel functional properties of Ca(2+) channel beta subunits revealed by their expression in adult rat heart cells. J. Physiol. *541*, 435–452.

Cooper, D.N., and Youssoufian, H. (1988). The CpG dinucleotide and human genetic disease. Hum. Genet. *78*, 151–155.

Ertel, E.A., Campbell, K.P., Harpold, M.M., Hofmann, F., Mori, Y., Perez-Reyes, E., Schwartz, A., Snutch, T.P., Tanabe, T., Birnbaumer, L., et al. (2000). Nomenclature of voltage-gated calcium channels. Neuron *25*, 533–535.

Faber, G.M., and Rudy, Y. (2000). Action potential and contractility changes in [Na(+)](i) overloaded cardiac myocytes: a simulation study. Biophys. J. *78*, 2392–2404.

Fombonne, E. (2003). Epidemiological surveys of autism and other pervasive developmental disorders: an update. J. Autism Dev. Disord. *33*, 365–382.

Goldin, A.L. (1991). Expression of ion channels by injection of mRNA into Xenopus oocytes. Methods Cell Biol. *36*, 487–509.

Hamill, O.P., Marty, A., Neher, E., Sakmann, B., and Sigworth, F.J. (1981). Improved patch-clamp techniques for high-resolution current recording from cells and cell-free membrane patches. Pflugers Arch. *391*, 85–100.

Herlitze, S., Hockerman, G.H., Scheuer, T., and Catterall, W.A. (1997). Molecular determinants of inactivation and G protein modulation in the intracellular loop connecting domains I and II of the calcium channel alpha1A subunit. Proc. Natl. Acad. Sci. USA *94*, 1512–1516.

Hurle, J.M., and Ganan, Y. (1986). Interdigital tissue chondrogenesis induced by surgical removal of the ectoderm in the embryonic chick leg bud. J. Embryol. Exp. Morphol. *94*, 231–244.

Imamura, S., Nishikawa, T., Hiratsuka, E., Takao, A., and Matsuoka, R. (2000). Behavior of smooth muscle cells during arterial ductal closure at birth. J. Histochem. Cytochem. *48*, 35–44.

Keating, M.T., and Sanguinetti, M.C. (2001). Molecular and cellular mechanisms of cardiac arrhythmias. Cell *104*, 569–580.

Korkman, M., Kirk, U., and Kemp, S. (1998). NEPSY: A Developmental Neuropsychological Assessment (San Antonio, TX: The Psychological Corporation).

Lee, K.S., Marban, E., and Tsien, R.W. (1985). Inactivation of calcium channels in mammalian heart cells: joint dependence on membrane potential and intracellular calcium. J. Physiol. *364*, 395–411.

Lord, C., Rutter, M., and Le Couteur, A. (1994). Autism Diagnostic Interview-Revised: a revised version of a diagnostic interview for caregivers of individuals with possible pervasive developmental disorders. J. Autism Dev. Disord. *24*, 659–685.

Lord, C., Risi, S., Lambrecht, L., Cook, E.H., Jr., Leventhal, B.L., DiLavore, P.C., Pickles, A., and Rutter, M. (2000). The autism diagnostic observation schedule-generic: a standard measure of social and communication deficits associated with the spectrum of autism. J. Autism Dev. Disord. *30*, 205–223.

Marks, M.L., Whisler, S.L., Clericuzio, C., and Keating, M. (1995). A new form of long QT syndrome associated with syndactyly. J. Am. Coll. Cardiol. *25*, 59–64.

Mikami, A., Imoto, K., Tanabe, T., Niidome, T., Mori, Y., Takeshima, H., Narumiya, S., and Numa, S. (1989). Primary structure and functional expression of the cardiac dihydropyridine-sensitive calcium channel. Nature *340*, 230–233.

Monnier, N., Procaccio, V., Stieglitz, P., and Lunardi, J. (1997). Malignant-hyperthermia susceptibility is associated with a mutation of the alpha 1-subunit of the human dihydropyridine-sensitive L-type voltage-dependent calcium-channel receptor in skeletal muscle. Am. J. Hum. Genet. *60*, 1316–1325.

Neyroud, N., Tesson, F., Denjoy, I., Leibovici, M., Donger, C., Barhanin, J., Faure, S., Gary, F., Coumel, P., Petit, C., et al. (1997). A novel mutation in the potassium channel gene KVLQT1 causes the Jervell and Lange-Nielsen cardioauditory syndrome. Nat. Genet. *15*, 186–189.

Ophoff, R.A., Terwindt, G.M., Vergouwe, M.N., van Eijk, R., Oefner, P.J., Hoffman, S.M., Lamerdin, J.E., Mohrenweiser, H.W., Bulman, D.E., Ferrari, M., et al. (1996). Familial hemiplegic migraine and episodic ataxia type-2 are caused by mutations in the Ca2+ channel gene CACNL1A4. Cell *87*, 543–552.

Orrenius, S., Zhivotovsky, B., and Nicotera, P. (2003). Regulation of cell death: the calcium-apoptosis link. Nat. Rev. Mol. Cell Biol. *4*, 552–565.

Priori, S.G., Aliot, E., Blomstrom-Lundqvist, C., Bossaert, L., Breithardt, G., Brugada, P., Camm, J.A., Cappato, R., Cobbe, S.M., Di, M.C., et al. (2002). Task Force on Sudden Cardiac Death, European Society of Cardiology. Europace *4*, 3–18.

Ptacek, L.J., Tawil, R., Griggs, R.C., Engel, A.G., Layzer, R.B., Kwiecinski, H., McManis, P.G., Santiago, L., Moore, M., Fouad, G., et al. (1994). Dihydropyridine receptor mutations cause hypokalemic periodic paralysis. Cell *77*, 863–868.

Reichenbach, H., Meister, E.M., and Theile, H. (1992). The heart-hand syndrome. A new variant of disorders of heart condition and syndactylia including osseous changes in hands and feet. Kinderarztl. Prax. *60*, 54–56.

Ren, D., Navarro, B., Perez, G., Jackson, A.C., Hsu, S., Shi, Q., Tilly, J.L., and Clapham, D.E. (2001). A sperm ion channel required for sperm motility and male fertility. Nature *413*, 603–609.

Sanguinetti, M.C., and Kass, R.S. (1984). Voltage-dependent block of calcium channel current in the calf cardiac Purkinje fiber by dihydropyridine calcium channel antagonists. Circ. Res. *55*, 336–348.

Schultz, D., Mikala, G., Yatani, A., Engle, D.B., Iles, D.E., Segers, B., Sinke, R.J., Weghuis, D.O., Klockner, U., Wakamori, M., et al. (1993). Cloning, chromosomal localization, and functional expression of the alpha 1 subunit of the L-type voltage-dependent calcium channel from normal human heart. Proc. Natl. Acad. Sci. USA *90*, 6228–6232.

Schulze-Bahr, E., Wang, Q., Wedekind, H., Haverkamp, W., Chen, Q., Sun, Y., Rubie, C., Hordt, M., Towbin, J.A., Borggrefe, M., et al. (1997). KCNE1 mutations cause Jervell and Lange-Nielsen syndrome. Nat. Genet. *17*, 267–268.

Shi, C., and Soldatov, N.M. (2002). Molecular determinants of voltage-dependent slow inactivation of the Ca2+ channel. J. Biol. Chem. *277*, 6813–6821.

Splawski, I., Timothy, K.W., Vincent, G.M., Atkinson, D.L., and Keating, M.T. (1997a). Molecular basis of the long-QT syndrome associated with deafness. N. Engl. J. Med. *336*, 1562–1567.

Splawski, I., Tristani-Firouzi, M., Lehmann, M.H., Sanguinetti, M.C., and Keating, M.T. (1997b). Mutations in the hminK gene cause long QT syndrome and suppress IKs function. Nat. Genet. *17*, 338–340.

Strom, T.M., Nyakatura, G., Apfelstedt-Sylla, E., Hellebrand, H., Lorenz, B., Weber, B.H., Wutz, K., Gutwillinger, N., Ruther, K., Drescher, B., et al. (1998). An L-type calcium-channel gene mutated in incomplete X-linked congenital stationary night blindness. Nat. Genet. *19*, 260–263.

Stuhmer, W. (1992). Electrophysiological recording from Xenopus oocytes. Methods Enzymol. *207*, 319–339.

Tananari, Y., Maeno, Y., Takagishi, T., Sasaguri, Y., Morimatsu, M., and Kato, H. (2000). Role of apoptosis in the closure of neonatal ductus arteriosus. Jpn. Circ. J. *64*, 684–688.

Tyson, J., Tranebjaerg, L., Bellman, S., Wren, C., Taylor, J.F., Bathen, J., Aslaksen, B., Sorland, S.J., Lund, O., Malcolm, S., et al. (1997). IsK and KvLQT1: mutation in either of the two subunits of the slow component of the delayed rectifier potassium channel can cause Jervell and Lange-Nielsen syndrome. Hum. Mol. Genet. *6*, 2179–2185.

Vitkup, D., Sander, C., and Church, G.M. (2003). The amino-acid mutational spectrum of human genetic disease. Genome Biol. *4*, R72. Published online October 30, 2003. 10.1186/gb-2003-4-11-r72

Volkmar, F.R., and Pauls, D. (2003). Autism. Lancet *362*, 1133–1141.

White, M.M., and Aylwin, M. (1990). Niflumic and flufenamic acids are potent reversible blockers of Ca2(+)-activated Cl- channels in Xenopus oocytes. Mol. Pharmacol. *37*, 720–724.

Zhang, J.F., Ellinor, P.T., Aldrich, R.W., and Tsien, R.W. (1994). Molecular determinants of voltage-dependent inactivation in calcium channels. Nature *372*, 97–100.

Zhang, L., Timothy, K.W., Vincent, G.M., Lehmann, M.H., Fox, J., Giuli, L.C., Shen, J., Splawski, I., Priori, S.G., Compton, S.J., et al. (2000). Spectrum of ST-T-wave patterns and repolarization parameters in congenital long-QT syndrome: ECG findings identify genotypes. Circulation *102*, 2849–2855.

Zheng, Z.J., Croft, J.B., Giles, W.H., and Mensah, G.A. (2001). Sudden cardiac death in the United States, 1989 to 1998. Circulation *104*, 2158–2163.

Zoghbi, H.Y. (2003). Postnatal neurodevelopmental disorders: meeting at the synapse? Science *302*, 826–830.